International Journal of Bioelectromagnetism *www.ijbem.org*
Vol. 23, No. 1, pp. 14/1 - 6, August 2021.

Real-time data processing for brain-computer interfacing using optically pumped magnetometers

J. Zerfowski[ab], T. H. Sander[a], M. Tangermann[c], S. R. Soekadar[b], T. Middelmann[a]
[a]*Physikalisch-Technische Bundesanstalt, Berlin, Germany*
[b]*Charité - Universitätsmedizin Berlin, Clinical Neurotechnology Laboratory, Berlin, Germany*
[c]*Donders Institute for Brain, Cognition and Behaviour, Radboud University, Nijmegen, The Netherlands*

Correspondence: Jan Zerfowski, Charitéplatz 1, 10117 Berlin
Email: jan.zerfowski@charite.de

Abstract. A brain-computer interface (BCI) translates brain signals into control commands of external devices. Compared to implantable BCIs, non-invasive systems based on electroencephalography (EEG) lack spatial resolution and signal bandwidth, e.g., to decode complex hand movements for high-dimensional control of an exoskeleton in paralysis. Here, we present a strategy for the real-time acquisition and analysis of neural data using optically pumped magnetometers (OPM) that promise to overcome these limitations. As a proof of concept, we implemented signal processing modules for real-time analysis of sensor data recorded by a 15-channel OPM grid placed over the occipital cortex. The modules filter and plot the data in the alpha frequency range and detect blockage of occipital alpha oscillations in real time. The processing stages are easily modifiable and allow for the implementation of different experimental paradigms. Establishing a flexible BCI framework for OPM-based magnetoencephalography (MEG) will not only improve versatility of BCIs, but will also pave the way to systematically investigate the neural substrates of BCI learning and BCI-triggered neuroplasticity.

Keywords: Optically pumped magnetometer, magnetoencephalography, brain-computer interface, exoskeleton control

1. Introduction

Optically pumped magnetometers (OPM) allow for noninvasive assessment of biomagnetic signals originating in the human cortex (Boto et al., 2016, Sander et al., 2020). Compared to cryogenic superconducting quantum interference devices (SQUID), OPMs offer a number of advantages: 1. OPMs work at room temperature reducing maintenance cost, 2. OPMs can be placed directly over the skull offering higher spatial resolution compared to SQUID-MEGs (Hill et al., 2020) and 3. OPMs are mobile allowing study participants to move freely in magnetically quiet environments. Moreover, compared to electroencephalography (EEG), OPMs do not require the use of conductive gels or other preparation procedures (impedance check, etc.). All these factors also facilitate application of OPM-MEG in children or study participants with difficulties to stay still.

Recent advancements in real-time signal processing enabled implementation of brain-computer interfaces (BCI) translating brain activity into control commands of external devices, e.g., prosthetics or exoskeletons (Soekadar et al., 2016). While BCIs were successfully implemented using various non-invasive recoding techniques, such as EEG, SQUID-MEG (Lal et al., 2005, Soekadar et al., 2011) or fNIRS (Soekadar et al., 2021), these non-invasive approaches are typically characterized by low spatial resolution limiting separation of signal sources for high-dimensional BCI control. Due to its increased spatial resolution compared to SQUID-MEG or EEG, OPM-MEG represents a very promising technique to overcome this limitation. It has been shown that real-time feedback can enable volitional control in stroke patients (Buch et al., 2008) (MEG) and full restoration of activities of daily living in patients with paralysis (Soekadar et al., 2019) (EEG). Common BCI paradigms classify movement intentions and other cognitive states by measuring the spectral power in particular frequency bands. For example, motor execution and motor imagery lead to a measurable decrease of signal power in alpha and beta bands (around 10 Hz and 20 Hz, respectively) over the motor cortex. This mechanism is called event-related (de)synchronization (ERD/ERS) and has become the basis for BCI approaches based on brain oscillations. ERD/ERS can be measured using EEG and has been used previously for exoskeleton hand control (Soekadar et al., 2015). Thanks to their potentially higher spatial resolution, it is hypothesized that OPM-MEG allows for better separation of different ERD sources compared to SQUID-MEG or EEG, and therefore enable higher degrees of freedom in future BCI applications. However, OPM-MEG-

based BCIs require the analysis of sensor data in real-time, which to our knowledge has not been achieved with an OPM sensor system yet.

Here, we present an analysis pipeline that interfaces OPM sensors from FieldLine Inc. with a total of 5 modular processing stages. It enables real-time acquisition, recording, pre-processing, classification and feedback of the incoming data. The pipeline executes a relatively simple thresholding of band power estimates from the occipital lobe while the study participant receives auditory cues to open and close their eyes. Good performance of such a pipeline is a prerequisite for further BCI paradigms as well as a proof-of-concept for real-time analysis of OPM-MEG signals in general.

2. Material and Methods

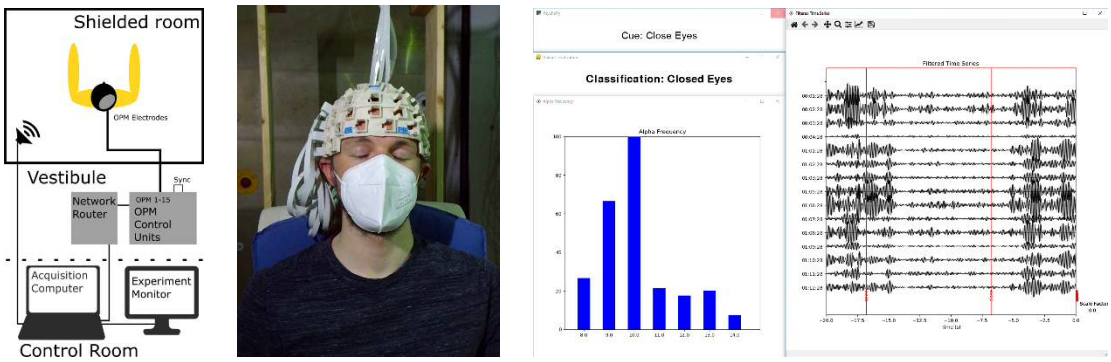

Figure 1. *(left)* ***Experimental setup.*** *The participant is wearing the OPM head mount inside a magnetically shielded room. Sensor cables are plugged into the sensor control units through small holes in the wall. A network router connects the OPM chassis with the acquisition and analysis computer. A piezoelectric speaker provides communication and auditory cues. (middle)* ***Photograph of a subject with closed eyes in the shielded room.*** *The helmet fixates the OPM sensors over the occipital cortex. (right)* ***View of analysis panel.*** *Left half shows condition information and classification results and a bar plot for averaged power in alpha frequency band. Right half visualizes alpha-bandpass filtered time series (8 Hz-14 Hz) in real-time over the last 20 seconds with red vertical lines marking condition changes.*

2.1. Hardware

We used 15 Rubidium vapor-based optically pumped magnetometers from FieldLine Inc. in the BMSR II magnetically shielded room (MSR) at the Physikalisch-Technische Bundesanstalt (PTB) in Berlin, Germany. Here, remnant magnetic fields are reduced to 0.5 nT (nanotesla) and it has a shielding factor above $1x10^8$ at 10 Hz and higher frequencies (Thiel et al., 2007). The OPMs operate in the spin-exchange relaxation free (SERF) regime (Kominis et al., 2003) and measure magnetic field changes originating from the human brain (Knappe et al., 2014). Since the SERF-regime relies on a residual field in the order of a few nanotesla, each sensor is equipped with an internal three-axis coil system to compensate for small remaining fields. The adjustment process of these fields is called “field-zeroing”. The sensors provide a bandwidth of more than 100 Hz with a noise floor at about 20 fT/√Hz. They were mounted in a helmet with a grid of slots such that the region of interest could be populated with several sensor units (Fig. 1). In our setup, the magnetometers were placed on the right occipital lobe over the visual cortex where the strongest alpha blockage can be observed when the eyes are open in comparison to when they are closed. Control data were recorded in a two-layer Ak3b MSR (VACUUMSCHMELZE GmbH & Co. KG) with active compensation and the results could be reproduced.

The magnetometers were connected to two sensor control units (11 + 4 sensors) outside the MSR. The control units were daisy-chained for automatic synchronization of their sampling intervals (Fig. 1). Through a networking router, the sensor control chassis were provided with an IP address and could consequently be discovered by other devices in the network. The manufacturer provides an application to start, calibrate and record data from the sensors, but the data can only be retrieved after the recording is stopped. To set up and control the sensors, an application programming interface (API) is supplied by FieldLine Inc. for python 3.8. It allows the user to manage the sensors and provides a callback interface which can be used to obtain the measured data in real-time. To present auditory cues for opening or closing the eyes, we used a piezoelectric speaker connected to the experiment control computer and the control room’s communication system.

2.2. LabStreamingLayer

The LabStreamingLayer (LSL) is a free and open-source implementation of a Transmission Control Protocol (TCP) stack that can be used to transmit and record data from multiple measurement devices. It permits synchronized processing of multiple data streams and avoids data loss by buffering on both the sender and receiver side. In principle, any time series and its metadata can be propagated between

applications and systems locally and on a network. The protocol is implemented by the cross-platform C++ library liblsl which provides an API to use functions defined in the protocol (e.g., sending data via "Outlets" and receiving data via "Inlets" in single samples or larger blocks). Samples can be supplemented with a system timestamp to achieve constant sampling rates and sub-millisecond timing precision even when the network transmission time is jittered. The user can specify the data type (e.g., EEG, MEG, other biosignals), number of channels, sampling rate through the stream's meta information which is shared with connected devices. Known delays between system clocks can also be taken into account by a delay parameter. Control and marker streams with non-constant sampling rates can be used to indicate the change of conditions, trials or as control commands. Wrappers for different programming languages (e.g., python, MATLAB, Java) offer an interface to the API and facilitate a wide array of use-cases for synchronized exchange of data. LSL is implemented natively by different device manufacturers and stimulation software packages (see here). However, none of the OPM-MEG systems we examined provide a way to stream the data via LSL.

2.3. Structure of the acquisition and analysis pipeline

To implement a structured acquisition, pre-processing and analysis pipeline in conjunction with stimulus presentation, we developed multiple independent modules. These modules use LSL for reliable and synchronized exchange of data and marker signals. Commonly, a distinction is made between data acquisition, data processing and feedback/stimulus presentation. To facilitate easy control of parameters between processing steps and offline analyses, we decided for a pipeline consisting of 6 modules (Fig. 2). Since the development of these modules was a major part of this project, we provide implementation details in the results section.

Acquisition. The first stage is responsible for data acquisition. It connects to the acquisition hardware units and publishes the acquired data via LSL. **Pre-processing.** The pre-processing module filters the sensor data in time and applies processing steps necessary for classification of the signal. **Classification.** A subsequent classification module receives the pre-processed data and returns its most likely class labels. It may express parameters such as thresholds adjustable by the experimenter or a stream Inlet for labels from the presentation module for model training. **Feedback.** In common BCI paradigms, the users control a particular variable or function while being able to observe their own performance in real-time. In our protocol, we only classified the eyes opened/closed state. Therefore, feedback was implemented only for the experimenter to check proper functioning of the pipeline. **Stimulus presentation.** The different experimental conditions must be conveyed to the study participant and marked accordingly in the data. Auditory cues were presented using PsychoPy (Peirce et al., 2019) and python scripting to publish condition changes. As noted above, the LSL stream can be used also in the classification node for training a corresponding classification algorithm. **Recording.** For later offline analyses and reproducibility, all stages of the data processing should be recorded synchronously. For this, the LabRecorder application provided with the LSL project is suggested.

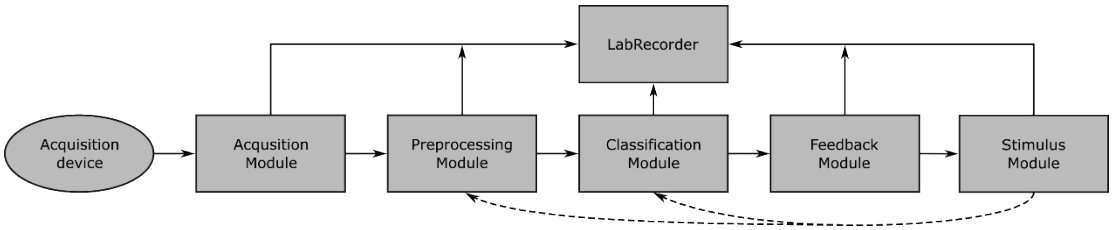

Figure 2. Processing pipeline depicting all stages of signal analysis. *Arrows represent direction of LSL streams. Dashed lines are optional associations between modules for plotting or classifier training. All modules propagate their data to the LabRecorder for recording.*

3. Results

In the following, we present the modules that were implemented for the acquisition and classification of the OPM data:

For the **data acquisition** module, we have built a command-line tool in python that acts as an interface between the API provided by FieldLine Inc. and the library pylsl. It automatically restarts the sensors, executes the field-zeroing steps and streams the data through an LSL outlet with metadata containing the sensor names and their configuration. The outlet can then be discovered on the network and the stream can be resolved by other applications and systems on the network to receive the samples. If single sensors fail during startup, the user is notified, and the data of the remaining sensors is streamed. The acquisition system has a fixed sampling rate of 1000 Hz and the API provides the data in blocks of 10 samples. Considering a theoretical network bandwidth of 1 Gbit/s, we do not expect issues concerning network speed or reliability even for several hundred sensors. Here, we only recorded the data of up to

15 OPM sensor channels. We did not experience delayed readout or timing problems using the reception timestamps of the acquisition computer.

We realized the **pre-processing** stage using NeuroPype, an application featuring a graphical "Pipeline Designer" to build and configure a pipeline that transforms and analyses the signal in real-time. It buffers incoming data and executes the processing nodes approximately 20 times per second. To extract the oscillatory alpha waves, we used a Butterworth IIR filter to bandpass filter the signal between 4 and 20 Hz. The signal was cropped to contain only the last 2000 ms of data and a standard FFT applied to analyze its spectrum. The data in frequency space was averaged over all channels and binned in steps of 1 Hz. To smoothen the signal, a moving average of 1.5 seconds was applied and the power estimates between 8 Hz-14 Hz were made available via LSL. We also plotted the filtered signal in real-time and scaled power estimates. This gives the experimenter a direct indication of data quality, participant compliance and pipeline functionality (Fig. 1).

A very simple **classifier** was achieved by thresholding the pre-processed signal. Frequency bins between 8 Hz and 14 Hz were multiplied by a Gaussian window centered around 11 Hz, summed and compared to a threshold value set by the experimenter. Since the participant did not receive any sensory BCI feedback in this specific setup, the **feedback** module was integrated into the classifier through a pygame-window displaying the current classification (Fig. 1).

For **stimulus presentation,** we used PsychoPy to play auditory cues to the participant over a speaker. Simple voice recordings were used to give the open/close eyes instructions. An LSL marker was sent to the pre-processing module immediately at condition change, which allowed displaying the marker in the time-series plot (Fig. 1).

To **record** the acquired signals together with condition markers, pre-processed data and classification results, the LabRecorder was used as suggested above. It allows to record available LSL streams on the network and can be controlled from the command line. The recordings were saved as xdf-files which also contain all streams' metadata and timestamps of the signal for later analyses.

The presented modules work independently, but together they form the processing pipeline depicted in Figure 2. Figure 1 shows how the time-series, experimental condition and classification/feedback stage can be monitored by the experimenter. The real-time processing and classification of the occipital alpha signal in closed/open eyes condition was run about 20 times per second and proved relatively high prediction accuracy (84%) after a small reaction time period (1.65 s) at condition change (Appendix 1).

4. Discussion

The pipeline presented above allows for real-time processing of brain signals recorded from an OPM-MEG system based on commercial sensors. The modularity of the processing stages and their independence enable easy replacement and adaptation of single parts for different experimental conditions or paradigms. Other data acquisition systems can be used if LSL functionality or real-time access to the data is provided.

In principle, a motor imagery BCI can be implemented with an altered processing pipeline, visual or haptic feedback and slight adaptation of the stimulus presentation. Stimulus presentation could be replaced using alternative software packages such as Neurobehavioral Systems' Presentation, Psychtoolbox or pygame and packages like numpy or Fieldtrip for data processing. Structured saving of channel metadata and time series in the xdf-format through LabRecorder permits subsequent offline analyses for larger studies and reproducibility of parameter settings.

5. Conclusion

In this work, we presented a processing pipeline for acquisition and classification of OPM-MEG sensor data recorded from the occipital cortex. The pipeline analyzes the data coming from a study participant's occipital lobe and provides instant feedback with an update rate of around 20 Hz. The timestamping functionality of LSL accounts for slight jitter in the operating system and network stack. Further, the signal can be recorded such that the resulting data of all processing stages are saved in synchrony and can be analyzed offline.

Prospectively, we aim to classify sensorimotor rhythm (SMR) ERD over the motor cortex with OPMs in an online setting that provides the user with real-time visual and proprioceptive feedback. After it was shown that EEG allows for control paradigms with only limited complexity (e.g., closing or opening an exoskeleton hand, controlling a cursor), we expect that the improved spatial resolution of OPM-MEG provides the necessary means to distinguish motor imagery of different body parts, for instance thumb and little finger, hand and elbow, or classification of different hand motions, e.g., grasping vs. pinching, etc. For these applications, improved separation of cortical signal sources may prove helpful. The use of co-registration procedures allowing for reproducible sensor localization in relation to the user's brain based on structural MRI images are already being investigated and promise to yield good results (Boto et al., 2016).

Acknowledgments

We wish to thank the LabStreamingLayer and pylsl developers for their fundamental work on the protocol and its implementation.

Appendix 1

To evaluate the prediction accuracy, we compared the time series of the eyes open and eyes closed conditions with the classifier output. The classifier runs at an update rate of about 20 Hz. Therefore, we implemented an offline analysis to compare the label of the classification (based on the last 2 seconds of data) with the actual condition label every 50 milliseconds. The reported accuracy reflects the ratio of 50 ms bins in which the correct class label (eyes open or closed) is estimated by the classifier. Since a delay between the auditory cue, the study participants closing their eyes and the onset of alpha can be expected, we analyzed the accuracy for shifts of the estimated labels against the correct labels within the interval of zero to five seconds. The maximum prediction accuracy can be seen for a shift of 1.65 seconds with a value of 0.84 or 84% (Fig. A2). It is important to note that this accuracy is based on short time windows. Integration over time or trial-based offline-classification could probably enhance accuracy substantially.

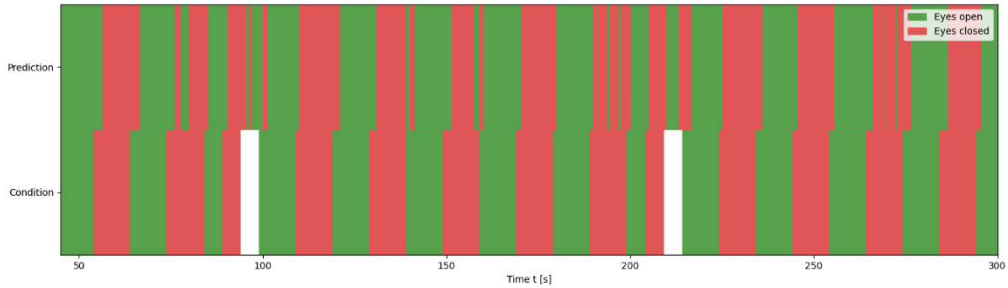

Figure A1. Condition label (bottom) and predicted label (top) for a representative subject. Green areas represent eyes open, red represents eyes closed. White spaces in the Condition timeline represent breaks between trials and were excluded from analysis. A short delay between upper and lower time series is clearly visible.

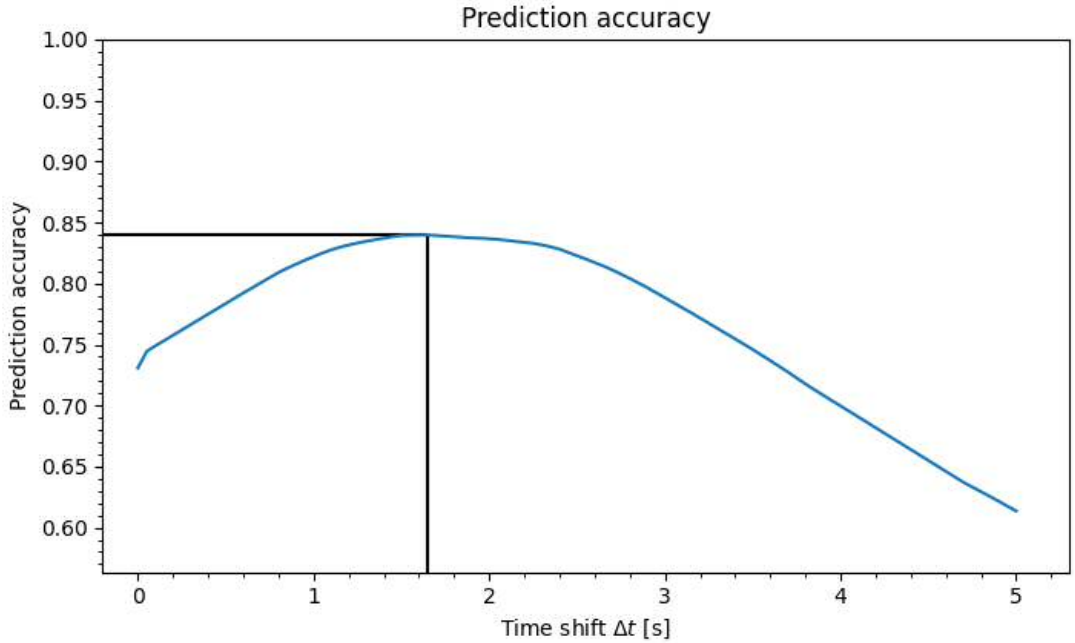

Figure A2. Prediction accuracy of the alpha power thresholding classifier as a function of time shift between predicted and correct condition label. For no shift the accuracy is about 73% and increases up to 84% at Δt=1.65 s. For larger Δt it decreases again monotonically. The black lines indicate the maximum accuracy.

References

Boto, E., Bowtell, R., Krüger, P., Fromhold, T. M., Morris, P. G., Meyer, S. S., Barnes, G. R., & Brookes, M. J. (2016). On the Potential of a New Generation of Magnetometers for MEG: A Beamformer Simulation Study. *PLOS ONE*, *11*(8), e0157655. https://doi.org/10.1371/journal.pone.0157655

Boto, E., Holmes, N., Leggett, J., Roberts, G., Shah, V., Meyer, S. S., Muñoz, L. D., Mullinger, K. J., Tierney, T. M., Bestmann, S., Barnes, G. R., Bowtell, R., & Brookes, M. J. (2018). Moving magnetoencephalography towards real-world applications with a wearable system. *Nature*, *555*(7698), 657–661. https://doi.org/10.1038/nature26147

Buch, E., Weber, C., Cohen, L. G., Braun, C., Dimyan, M. A., Ard, T., Mellinger, J., Caria, A., Soekadar, S., Fourkas, A., & Birbaumer, N. (2008). Think to move: A neuromagnetic brain-computer interface (BCI) system for chronic stroke. *Stroke*, *39*(3), 910–917. https://doi.org/10.1161/STROKEAHA.107.505313

Hill, R. M., Boto, E., Rea, M., Holmes, N., Leggett, J., Coles, L. A., Papastavrou, M., Everton, S., Hunt, B. A. E., Sims, D., Osborne, J., Shah, V., Bowtell, R., & Brookes, M. J. (2020). *Multi-Channel Whole-Head OPM-MEG: Helmet Design and a Comparison with a Conventional System*. https://doi.org/10.1101/2020.03.12.989129

Knappe, S., Sander, T., & Trahms, L. (2014). Optically-Pumped Magnetometers for MEG. In S. Supek & C. J. Aine (Eds.), *Magnetoencephalography* (pp. 993–999). Springer Berlin Heidelberg. https://doi.org/10.1007/978-3-642-33045-2_49

Kominis, I. K., Kornack, T. W., Allred, J. C., & Romalis, M. V. (2003). A subfemtotesla multichannel atomic magnetometer. *Nature*, *422*(6932), 596–599. https://doi.org/10.1038/nature01484

Lal, T. N., Birbaumer, N., Schölkopf, B., Schröder, M., Hill, N. J., Preissl, H., Hinterberger, T., Mellinger, J., Bogdan, M., Rosenstiel, W., & Hofmann, T. (2005). A brain computer interface with online feedback based on magnetoencephalography. *Proceedings of the 22nd International Conference on Machine Learning - ICML '05*, 465–472. https://doi.org/10.1145/1102351.1102410

Peirce, J., Gray, J. R., Simpson, S., MacAskill, M., Höchenberger, R., Sogo, H., Kastman, E., & Lindeløv, J. K. (2019). PsychoPy2: Experiments in behavior made easy. *Behavior Research Methods*, *51*(1), 195–203. https://doi.org/10.3758/s13428-018-01193-y

Sander, T., Jodko-Władzińska, A., Hartwig, S., Brühl, R., & Middelmann, T. (2020). Optically pumped magnetometers enable a new level of biomagnetic measurements. *Advanced Optical Technologies*, *9*, 247–251. https://doi.org/10.1515/aot-2020-0027

Soekadar, S. R., Witkowski, M., Gómez, C., Opisso, E., Medina, J., Cortese, M., Cempini, M., Carrozza, M. C., Cohen, L. G., Birbaumer, N., & Vitiello, N. (2016). Hybrid EEG/EOG-based brain/neural hand exoskeleton restores fully independent daily living activities after quadriplegia. *Science Robotics*, *1*(1). https://doi.org/10.1126/scirobotics.aag3296

Soekadar, Surjo R., Kohl, S. H., Mihara, M., & von Lühmann, A. (2021). Optical brain imaging and its application to neurofeedback. *NeuroImage. Clinical*, *30*, 102577. https://doi.org/10.1016/j.nicl.2021.102577

Soekadar, Surjo R., Nann, M., Crea, S., Trigili, E., Gómez, C., Opisso, E., Cohen, L. G., Birbaumer, N., & Vitiello, N. (2019). Restoration of Finger and Arm Movements Using Hybrid Brain/Neural Assistive Technology in Everyday Life Environments. In C. Guger, N. Mrachacz-Kersting, & B. Z. Allison (Eds.), *Brain-Computer Interface Research* (pp. 53–61). Springer International Publishing. https://doi.org/10.1007/978-3-030-05668-1_5

Soekadar, Surjo R., Witkowski, M., Vitiello, N., & Birbaumer, N. (2015). An EEG/EOG-based hybrid brain-neural computer interaction (BNCI) system to control an exoskeleton for the paralyzed hand. *Biomedical Engineering / Biomedizinische Technik*, *60*(3), 199–205. https://doi.org/10.1515/bmt-2014-0126

Soekadar, Surjo R., Witkowski, M., Mellinger, J., Ramos, A., Birbaumer, N., & Cohen, L. G. (2011). ERD-Based Online Brain–Machine Interfaces (BMI) in the Context of Neurorehabilitation: Optimizing BMI Learning and Performance. *IEEE Transactions on Neural Systems and Rehabilitation Engineering*, *19*(5), 542–549. https://doi.org/10.1109/TNSRE.2011.2166809

Thiel, F., Schnabel, A., Knappe-Grüneberg, S., Stollfuß, D., & Burghoff, M. (2007). Demagnetization of magnetically shielded rooms. *Review of Scientific Instruments*, *78*(3), 035106. https://doi.org/10.1063/1.2713433